Food and Chemical Toxicology 188 (2024) 114627

Contents lists available at ScienceDirect

Food and Chemical Toxicology

journal homepage: www.elsevier.com/locate/foodchemtox

Gut-gonad crosstalk in mice exposed to a "chemical cocktail" combining metabolomics and microbial profile by amplicon sequencing

C. Parra-Martínez [a], M. Selma-Royo [b], B. Callejón-Leblic [a], M.C. Collado [b,1], N. Abril [c,1], T. García-Barrera [a,*,1]

[a] Research Center of Natural Resources, Health and the Environment (RENSMA), Department of Chemistry, Faculty of Experimental Sciences, University of Huelva, Fuerzas Armadas Ave., 21007, Huelva, Spain
[b] Institute of Agrochemistry and Food Technology-National Research Council (IATA-CSIC), Agustin Escardino 7, 46980, Paterna, Valencia, Spain
[c] Department of Biochemistry and Molecular Biology, University of Córdoba, Campus de Rabanales, Edificio Severo Ochoa, E-14071, Córdoba, Spain

ARTICLE INFO

Handling Editor: Bryan Delaney

Keywords:
Testicular metabolomics
Selenium
Chemical cocktails
Metallomics
Microbiota

ABSTRACT

Testes are very prone to be damaged by environmental pollutants, but there is a lack of information about the impact of "chemical cocktails" (CC) on the testicular metabolome and the possible influence in the gut-gonad crosstalk. For this, BALB/c mice were given flumequine and diclofenac orally in food and potentially toxic trace elements (Cd, Hg, As) in drinking water. A mice group was supplemented with selenium, a well-known antagonist against many pollutants. Our results revealed that the steroid 5-alpha-androstan-17-beta-ol propionate, suggested as a parameter of androgenicity independent of testosterone levels, proline that improves reproductive indicators in male rabbits affected by environmental stress) among others metabolites are only present after CC exposure with rodent and selenium supplemented diet. Selenium also antagonized the up-or down-regulation of anandamide (20:l, n-9) ($p < 0.001$ and FC 0.54 of CC vs C but $p > 0,05$ and FC 0.74 of CC-Se vs C), that regulates gonadotropin-releasing hormones in mammals, 2,3-dinor-11b-PGF2a ($p < 0.001$ and FC 0.12 of CC vs C but $p > 0,05$ and FC 0.34 of CC-Se vs C), which has been related with reproductive hormones, besides others testicular metabolites altered by the exposure to the CC and reversed the levels to control. Moreover, numerous significant associations between gut microbes and testicular metabolites indicated a possible impact of pollutants in the testes mediated by gut microbiota due to a gut-gonad crosstalk.

1. Introduction

According to a recent report published in 2018 on assisted reproductive techniques in the European Union for the year 2014, there is a clear trend showing a continuous expansion of the number of reproductive treatments in Europe (De Geyter et al., 2018). In parallel, there is a continuous upward trend of the infertility rate in this century being about 15% of couples infertile and about 40–50% of infertility cases caused by males (Kilchevsky and Honig, 2012). The causes of male infertility are multifaceted and the etiology of a high percentage of cases remains unknown, but concerns have arisen regarding the impact of environmental pollutants (Gao et al., 2015). Among them, mercury (Hg) exposure can disrupt the reproductive system and induce immunosuppression, fibrosis (Li et al., 2022) and metabolic impairments in male mice (M. A. García-Sevillano et al., 2014), arsenic (As) can affect spermatogenesis and testicular morphologic structure, leading to oxidative stress (Wu et al., 2021), metabolic impairments (García-Sevillano et al., 2013a) and inducing a gradual reduction in Leydig cell population (da Silva et al., 2017; Sarkar et al., 2008) and spermatozoa (da Silva et al., 2017), while cadmium (Cd) can damage germ and Sertoli cells, and produce testicular necrosis, since this metal leads to the rupture of the blood-testis barrier (Minutoli et al., 2015). However, synergistic and antagonistic effects between pollutants have been frequently described (García-Barrera et al., 2012; García-Sevillano et al., 2013b; M. Á. García-Sevillano et al., 2014b, 2014a; Rodríguez-Moro et al., 2019), and thus, their biological effect should not be studied in isolation. Likewise, zinc (Zn) can protect testicular damage caused by low-dose of Hg in mice (Orisakwe et al., 2001), As and antimony (Sb) can cause synergistic toxic effects in mice testis (Wu et al., 2021), while selenium (Se) can attenuate diclofenac (DCF)-induced testicular and

* Corresponding author.
E-mail address: tamara@dqcm.uhu.es (T. García-Barrera).
[1] Senior authors.

https://doi.org/10.1016/j.fct.2024.114627
Received 8 January 2024; Received in revised form 27 February 2024; Accepted 28 March 2024
Available online 30 March 2024

epididymal toxicity in rats (Owumi et al., 2020) and it is well-known for its antagonistic action against many other pollutants (García-Barrera et al., 2012). Due to the health-relevant effects of Se, it has been proposed as a functional supplement (Gómez-Jacinto et al., 2012) as well as for preventing several diseases like cancer (Cai et al., 2016).

In addition, "chemical cocktails" can shape gut microbiota (Arias-Borrego et al., 2022; Ramírez-Acosta et al., 2021) and brain metabolome (Parra-Martínez et al., 2022), while Se modulates the gut microbiota towards an increase in some potencially beneficial microorganisms (*e.g. Lactobacillus* genus) (Callejón-Leblic et al., 2021) and shapes gut metabolites (Callejón-Leblic et al., 2022).

Previous studies, including Jarak et al. (2018), have identified a diverse range of metabolites within the rat testis, highlighting the presence of amino acids, their derivatives, organic acids, lipid-related compounds, and nitrogenous bases. Notably, pathways involved in phospholipid, nucleotide, and amino acid metabolism, alongside energy-generating pathways like the TCA cycle, glycolysis, and glyoxylate and dicarboxylate metabolism, stand out as key players in testicular function.

Herein, we described the impact of a "chemical cocktail" of potentially toxic trace elements (As, Cd, Hg) and pharmaceuticals (DCF and flumequine, FLQ) on mice testicular metabolome and the potential communication with the gut microbiota. Moreover, a group of mice was supplemented with Se to delve into the potential antagonism against those pollutants.

2. Experimental section

2.1. Experimental design with mice and dosage information

The experiments with animals were performed at the Animal Experimentation Service of the University of Cordoba (SAEX-UCO), by qualified staff and following the European Community animal care guidelines. This work has been approved by the research ethics from Ethical Committee of the University of Córdoba and the Regional Government of Andalusia (Spain) and a proof/certificate is available on request (Code Num. October 17, 2022/126). The experimental design has been previously described (Arias-Borrego et al., 2022). Briefly, eight weeks *Mus musculus* BALB/c male mice were randomly divided into three groups for three weeks (n = 12) and they were housed in pairs under controlled laboratory conditions, with free access to food and water (Arias-Borrego et al., 2022). Control group (C) was fed a rodent diet, the group CC received a "chemical cocktail" of DCF and FLQ in the chow as well as Arsenic trioxide, Mercury (II) chloride and Cadmium chloride in the drinking water, and the group CC-Se received the "chemical cocktail", but also a Se-supplemented show with a Se-dosage according to previous studies (D'Amato et al., 2020; Zarrinpar et al., 2018). The dosages for pollutants were based on concentrations of environmental relevance (Fekadu et al., 2019; González-Gaya et al., 2022; Huygens et al., 2022). Fig. 1 summarizes the exposure experiment.

2.2. Extraction of metabolites from testicular tissues

Metabolites were extracted from testicular tissues following a previously described sample treatment (Ramírez-Acosta et al., 2023). Briefly, the testicular tissues were cryohomogenized using liquid nitrogen into a ceramic mortar. Then, 30.0000 mg of sample were mixed with cold methanol/water (1:1, v/v, −20 °C) into a 2 mL cryotube of a TissueLyser LT homogenizer (Qiagen, Germany). A volume of 100 μL was treated with 400 μL of methanol/methyl *tert*-butyl ether (MTBE) (80:20, *v/v*) and vortex-mixed during 1h. Afterward, the extracts were centrifuged at 4000 *g* at 20 °C for 20 min and the supernatants were divided in two exact aliquots for the analysis by gas chromatography coupled to mass spectrometry (GC-MS) and ultra-high performance liquid chromatography coupled to quadrupole time of flight mass spectrometer (UHPLC-QTOF). The extracts were dried into a SpeedVac concentrator system at 35 °C (Thermo Fisher Scientific, Bremen, Germany). For UHLC-QTOF analysis, the extracts of metabolites were reconstituted using a mixture of methanol/MTBE (80:20, *v/v*) and then, 10 μL were injected into the UHPLC loop. The analysis by GC-MS required a derivatization procedure that consisted of two steps: (i) methoxymation, by adding to the dried extracts 50 μL of methoxyamine hydrochloride in pyridine (20 mg mL^{-1}), which was later incubated at 80 °C during 15 min, to protect carbonyl groups. (ii) Silylation, by adding N-methyl-N-(trimethylsilyl)trifluoroacetamide (50 μL), which was later incubated under the same conditions used in the methoxymation. The reproducibility and stability of the analysis were assured by preparing six pools with equal volumes of testicular extracts quality control (QCs).

2.3. Quality control samples preparation

For each matrix, a total of six Quality Control samples (QCs) were prepared by pooling equal volumes (20 μl) of all brain extracts from each mice in the study, which were treated with the sample procedure and analyzed for UPLC-QTOF-MS and GC–MS. Quality controls results were statistically treated by principal component analysis (PCA) and score plots represented to check the stability during the analysis". The relative standard deviation of QC for each metabolite are shown in the supplementary material (Table S1).

2.4. GC-MS metabolomic analysis

The chromatographic separation of metabolites was carried out into

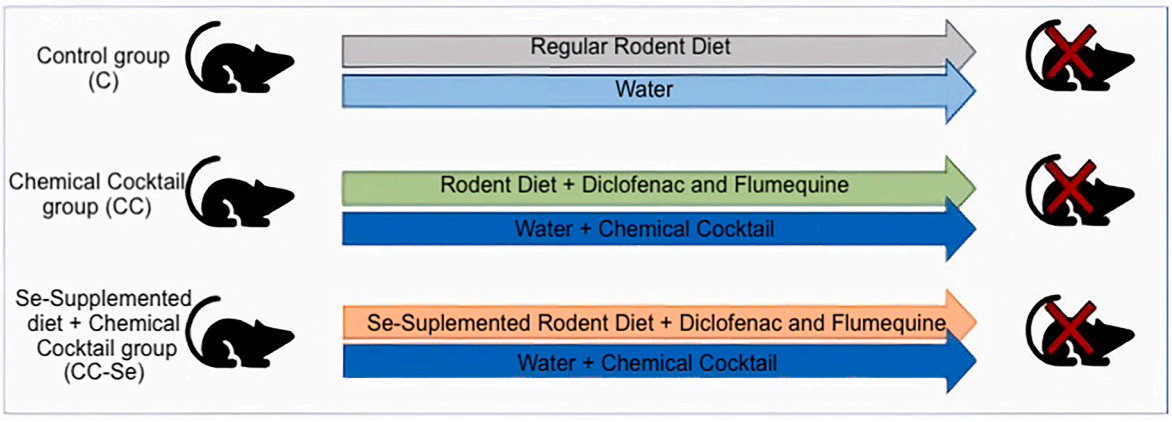

Fig. 1. Experimental design for the animal exposure experiment.

a GC-MS ion trap model Trace GC ULTRA ITQ900 (Thermo Fisher Scientific), using a VF-5MS Factor Four column with dimensions 30 m × 0.25 mm, 0.25 μm (Agilent technologies, Tokyo, Japan) and helium at 1 mL min^{-1} as carrier gas. A volume of 1 μL of the derivatized extract was injected into the oven at 200 °C. The temperature of the GC oven was ramped from 100 °C (maintained 0.5 min) to 320 °C at 15 °C min^{-1} (2.8 min). Metabolites were ionized at 70 eV by electronic impact and the filament was turned off during the first 4 min. MS spectra were acquired in from 35 to 650 m/z.

2.5. UHPLC-QTOF metabolomic analysis

An IM-QTOF model 6560 Ion Mobility LC/Q-TOF system with a dual electrospray ion source handled in both positive and negative ionization modes (Agilent Technologies, Tokyo, Japan) was used and coupled to a 1290 Agilent UHPLC. Metabolites were separated by reversed-phase chromatography at 0.4 mL min^{-1} using a gradient from 5 to 95% of the organic mobile phase (acetonitrile) that was mixed with a second aqueous mobile phase, both with 0.5% (v/v) formic acid. The injection volume was 10 μL and the separation was carried out into a chromatographic column model Agilent Zorbax Eclipse Plus C18 with dimensions of 50 × 2.1 mm, 1.8 μm. The temperature of the column was maintained at 45 °C. Reference masses were introduced for mass calibration in positive (121.0509 and 922.0098 m/z) and negative (1033.9881 and 112.9856 m/z) ionization modes. Other parameters are described in the supplementary material (Table S1).

2.6. Annotation of testicular tissue metabolites

GC-MS data were turned into.CDF files utilizing the Thermo File Converter tool (Thermo Fisher Scientific). We used XCMS software included in the R platform (http://www.r-project.org) for the extraction, peaks alignment and data normal standardization. In this sense, information were obtained by utilizing the calculation "matched filter method" what cuts the information into extracted ion chromatograms (XIC) on a firm step size, and afterward each cut was sifted with matched filtration utilizing a second-subsidiary Gaussian as the model peak shape. The data extraction parameters for GC–MS files were S/N threshold 2, full width at half-maximum (fwhm) 3, and width of the m/z range 0.1. After peak extraction, three iterative cycles with descending bandwidth (bw) from 5 to 1 s were used for grouping and retention time correction. To normalize the data we performed the locally weighted scatter plot smoothing (LOESS) method, which adjusts the local median of log fold changes of peak intensities between samples in the dataset to be approximately zero across the whole peak intensity range. Then, we exported the preprocessed data as a.csv file due to perform further statistical analysis.

We processed the UHPLC-QTOF-MS raw data with Agilent MassHunter Profinder B.10.0 software (Agilent Technologies). We used the Recursive Feature Extraction (RFE) for small molecules from the software to extract de data. RFE consists of two algorithms: First, Molecular Feature Extraction (MFE), which uses extraction, selection of ion species, and charge state to find the features in the dataset. Then, the initial features were aligned by retention time (RT) and mass to create a list of unique features through binning. Second, we performed the Find by Ion algorithm (FbI) using the RT and mass data pairs of the aligned and binning features as input criteria to find the features more accurately. Scoring, integration, and peak filters were also applied as additional filters to the dataset. We used Mass Profiler Professional B.10.0 (Agilent Technologies) to normalize the dataset using total area sums (Supporting information, Table S1).

In order to statistically process the GC-MS data the software SIMCA-P™ (version 11.5, published by UMetrics AB, Umeå, Sweden) was used, features were filtered according to the Variable Importance in the Projection (VIP), taking into account only variables with VIP values above 1.5, which is a good indicative of significant differences among groups.

Mass Profiler Professional B.10.0 (Agilent Technologies) was used to process the data obtained from UHPLC-QTOF-MS, resulting in the determination of the most relevant metabolites between groups. Principal component analysis (PCA) and partial least squares discriminant analysis (PLS-DA) were carried out for the statistically relevant features found in UHPLC-QTOF-MS and GC-MS. The software supplied us with the predictive and class separation parameters R2 and Q2 of all models built. Before performing statistical analysis, Pareto scaling and logarithmic transformation were applied to the data.

STATISTICA 8.0 from StatSoft was the software used to obtain one-way ANOVA and Tukey test for multiple comparisons. Besides, p-values were adjusted with a Benjamin Hochberg FDR correction. On the other hand, we used R Software Package Hmisc (4.0.2 version) to determine Spearman correlations between gut metabolites and microbiota at the genus level and to plot the heatmaps. The level of statistical significance for all tests was set to $p < 0.05$.

For GC-MS metabolomic analysis, version 8 NIST Mass Spectral Library was used to annotate metabolites, selecting only those with a probability >80%. Target ions and at least two qualifiers (identifier ions) were selected from each mass spectrum. Those metabolites with a variation of less than 20% in the area qualifier/target ion ratio per metabolite were selected. Kovat's retention indexes (KRI) were calculated for the metabolites using a mixture of alkanes from C7–C40 (Sigma Aldrich, Germany). For UHLC-QTOF-MS metabolomic analysis, the software MassHunter version B.08.00 was used. To this end, the workflow "Compound Discovery" and the compound mining "Find by Molecular Features" were applied to the dataset. METLIN (http://metlin.scripps.edu) and HMDB (http://hmdb.ca) databases were used considering only those metabolites with a score higher than 90%. In addition, MS-MS experiments were performed with the same experimental conditions as applied for the primary analysis. Collision-induced dissociation (CID) fragmentation was used.

2.7. Gut microbiota profiling

The gut microbiota profile was obtained by 16S rRNA V3–V4 amplicon sequencing following Illumina protocols as previously described (Arias-Borrego et al., 2022). Previous data was used to identify specific associations between testicular tissue metabolites and gut microbes. As described previously, sequences were processed a with the DADA2 pipeline and taxonomy was assigned with the Silva v132 database. Tables with taxonomy at different levels (phylum, family, and genus) were used to combine with the available data in this study.

3. Results

3.1. Testicular mouse metabolome after exposure to the "chemical cocktail" and selenium supplementation

The mice groups studied (C, CC, and CC-Se) were grouped and separated according to their testicular metabolome as can be seen in the principal least squares discriminant analysis plots (PLS-DA) using GC-MS (Fig. 2A), UHPLC-($^{+}$ESI)-QTOF (Fig. 2B) and UHPLC-($^{-}$ESI)-QTOF (Fig. 2C). GC-MS led to the poorer separation between groups, probably due to the few number of metabolites annotated with this analytical technique. However, the separation between groups was much better by using UHPLC-QTOF with both ionization modes. Under these conditions, the C group presented the most difference, while CC and CC-Se were only partially separated indicating a partial antagonistic effect of Se-supplementation in the mice's testicular metabolome after the exposure to the CC. Principal components analysis (PCA) (Fig. S1) showed a perfect clustering of the QCs indicating a good reproducibility and stability of the analysis. The partial least squares discriminant analysis (PLS-DAs) built for pairwise comparisons between the studied groups are shown in Fig. S2.

After the analysis, 41 testicular metabolites were annotated

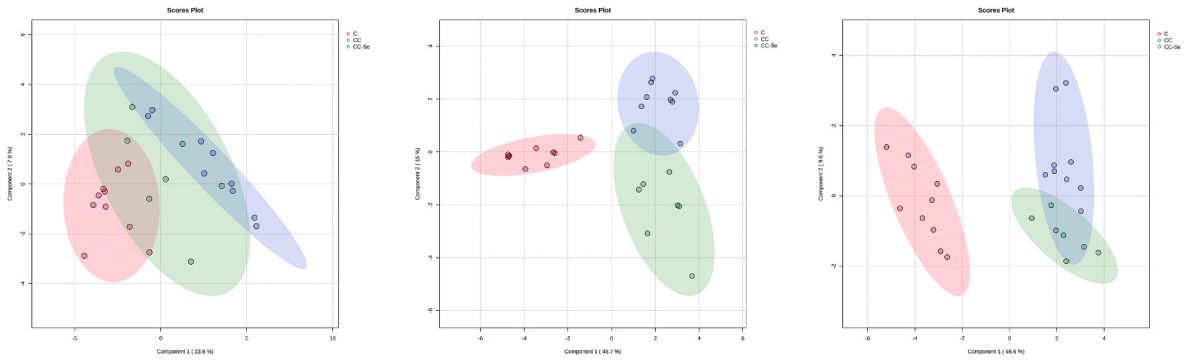

Fig. 2. (A) 3D-PLS-DA of testicular samples corresponding to GC-MS analysis, (B) UHPLC-ESI^{+}-QTOF-MS and (C) UHPLC-ESI^{-}-QTOF-MS. C: red dots, CC: green dots, CC-Se: blue dots. (For interpretation of the references to color in this figure legend, the reader is referred to the Web version of this article.)

(Table S2) in the different studied groups using GC-MS (11 metabolites) and UHPLC-($^{+/-}$ESI)-QTOF (30 metabolites). The *p*-values and fold-changes (FC) of their relative abundance were also calculated for each metabolite in testicular tissue after the comparison of the groups CC and CC-Se with C (Table S2). The FC showed several metabolites that were up-regulated and others down-regulated when comparing the CC and CC-Se groups with C. Table S3 collects the Kovat's retention index (KRIs) of each metabolite annotated by GC-MS as well as the number of trimethylsilyl groups attached to the metabolite (X-TMS), retention times and targeted/qualifier ions used. Fig. 3 shows a heatmap diagram with the list of metabolites annotated and their relative abundance in the different groups. As can be seen (Table S2), **there was a group of metabolites that were not detectable in mice testes of the control group** and for this reason, it was not possible to calculate the FC (CC *vs* C nor CC-Se *vs* C). However, **their relative abundance in testicular tissue was different in mice supplemented with Se or rodent diet**. This group includes (compound class, FC CC-Se *vs* CC): FLQ (quinolones and derivatives, 2.36-fold), nordihydrocapsiate (phenols, 1.69-fold), proline (carboxylic acid and derivatives, 3.84-fold) and 5-alpha-Androstan-17-beta-ol propionate (steraloid, 0.09-fold). **Other metabolites were absent in the control group, but there were not significant change in their abundance when comparing CC with CC-Se**: Lysophosphatidylethanolamine (LysoPE) (16:0) (glycerophospholipid) and N-(14-methylhexadecanoyl) (pyrrolidines).

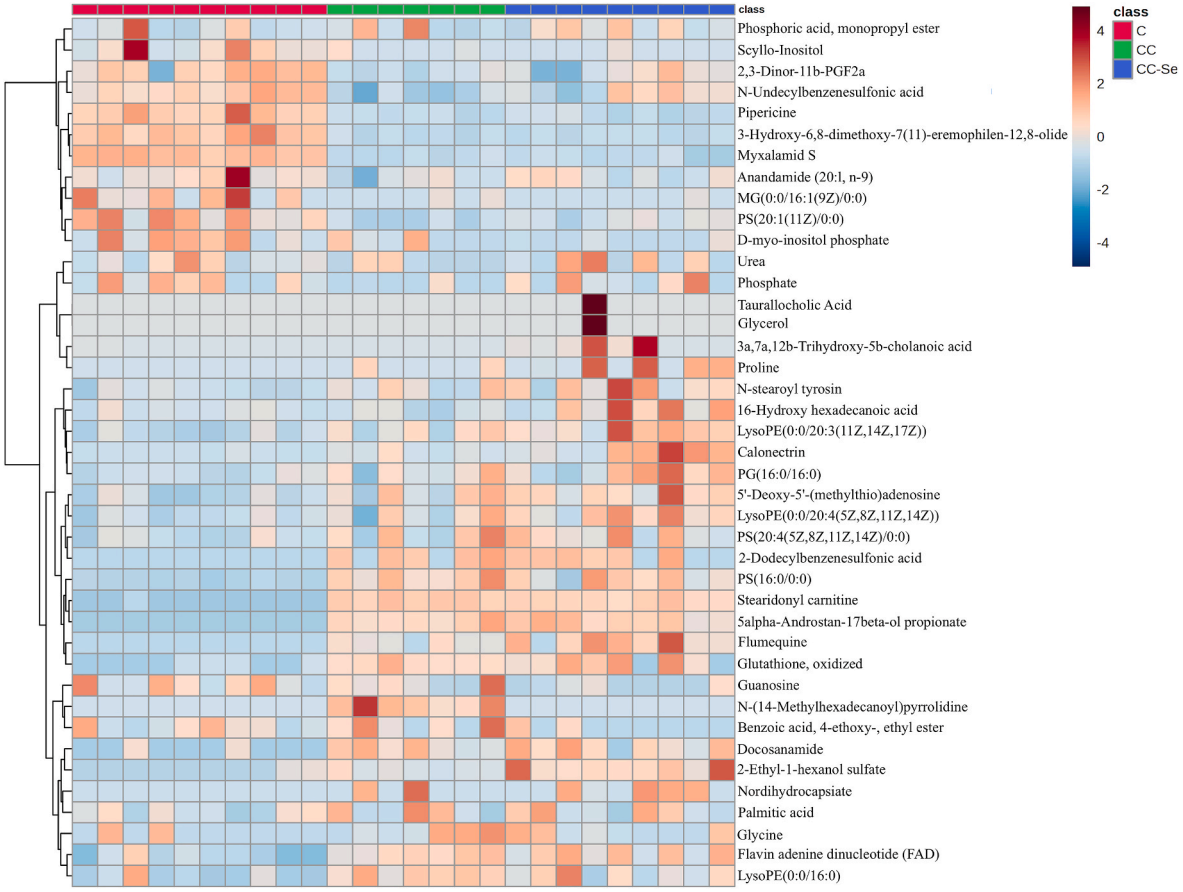

Fig. 3. Cluster heatmap of testicular metabolites from C, CC and CC-Se mice. Metabolites are represented in rows and mice of different groups in columns. Red and blue colors show increased and decreased levels of testicular metabolites, respectively. (For interpretation of the references to color in this figure legend, the reader is referred to the Web version of this article.)

Interestingly, there is also a group of metabolites that was altered after CC exposure, but Se-supplementation restored their abundance similar to the control group (not significant change in their abundance when comparing CC-Se *vs* C). This group includes (compound class and FC for CC *vs* C in brackets): anandamide (20:1, n-9) (organonitrogen compounds, 0.54-fold), 2,3-Dinor-11b-PGF2a (fatty acyl, 0.12-fold), PG(16:0/16:0) (glycerophospholipid, 1.57-fold), and N-undecylbenzenesulfonic acid (benzene and substitute derivative, 0.45-fold). Likewise, **there was another band of metabolites that were up- or down-regulated in mice testes after the CC exposure and Se-supplementation led to the opposite regulation**. This group includes (compound class, FC CC *vs* C, CC-Se *vs* C): taurallocholic acid (steroids and steroid derivatives, 0.37-fold, not calculable because absent in one group) and glycerol (organooxygen compounds, not calculable because absent in one group). Finally, **there is a group of metabolites up- or down-regulated after CC exposure and Se-supplementation that were not impaired in the CC group** that includes (FC CC-Se *vs* C): 5′-deoxy-5'-(methylthio)adenosine (5′-deoxyribonucleosides, 1.59-fold), 3a,7a,12b-trihydroxy-5b-cholanoic acid (organooxygen compound, 30.71-fold), LysoPE(20:3) (glycerophospholipid, 1.63-fold), LysoPE (20:4) (glycerophospholipid, 1.52-fold), myxalamid S (0.16-fold), PS (20:4) (glycerophospholipids, 1.59-fold), N-stearoyl tyrosine (carboxylic compounds and derivatives, 3.27-fold), calonectrin (prenol lipids, 3.11-fold), MG(16:1) (glycerolipid, 0.04-fold), 16-hydroxy hexadecanoic acid (fatty acyls, 1.38-fold).

As can be seen (Fig. 3, Table S2), **there was a band of metabolites that is down-regulated in mice testes after the exposure to the CC and even after Se-supplementation**. This group includes metabolites as (compound class and FC for CC *vs* C and CC-Se *vs* C, respectively, in brackets): pipericine (fatty acyl, 0.27-fold, 0.26-fold), 3-hydroxy-6,8-dimethoxy-7(11)-eremophilen-12,8-olide (organooxygen compound, 0.12-fold, 0.14-fold), myxalamid S (lipid, 0.18-fold, 0.16-fold), Guanosine (purines, 0.02-fold, 0.01-fold), Palmitic acid (lipid, 0.21-fold, 0.27-fold), carbamide (amide, 0.3-fold, 0.36-fold), Ethyl 4-ethoxybenzoate (Benzene derivative, 0.85-fold, 0.86-fold), Phosphoric acid, monopropyl ester (Phosphate ester, 0.58-fold, 0.71-fold) and monoglyceride (MG) (16:1) (glycerolipid, 0.13-fold, 0.04-fold). **Otherwise, there is also a band of compounds that was up-regulated in the mice testes after the exposure to the CC and even after Se-supplementation**. This group includes: FLQ (quinoline carboxylic acid, not present in C), phosphatidylserine (PS) (16:0) (glycerophospholipid, 4.64-fold, 3.79-fold), flavin adenine dinucleotide (flavin nucleotide, 2.7-fold, 2.8-fold), stearidonyl carnitine (fatty acyl, 47.04-fold, 42.48-fold), docosanamide (fatty acyl, 6.02-fold, 6.20-fold), PS(20:4) (glycerophospholipid, 1.52-fold, 1.58-fold), Lyso phosphatidylethanolamine (LysoPE) (16:0) (glycerophospholipid, 2.87-fold, 3.35-fold), oxidized glutathione) (carboxylic acids and derivatives, 2.81-fold, 2.10-fold), PS(20:1) (glycerophospholipid, 7.25-fold, 7.14-fold), LysoPE(16:0) (glycerophospholipid, not calculable because absent in one group), 5-alpha-Androstan-17-beta-ol propionate (steroid, not calculable because absent in one group), 2-ethyl-1-hexanol sulfate (organic sulfuric acids and derivatives, 4.00-fold, 10.72-fold), phosphatidylglycerol (PG) (16:0/16:0) (glycerophospholipid, 1.57-fold, 2.14-fold), nordihydrocapsiate (phenol, not calculable because absent in one group), glycine (carboxylic compounds and derivatives, 4.38-fold, 2.28-fold), proline (carboxylic compounds and derivatives, not calculable because absent in one group).

The altered metabolic pathways in mice testes after CC exposure and Se-supplementation were evaluated using the MetaboAnalyst 5.0 tool (metaboanalyst.ca). Fig. 4A and Table S4 show that three metabolic pathways were significantly impaired after CC exposure when the metabolome is compared with C, namely: glutathione metabolism, aminoacyl-tRNA biosynthesis, riboflavin metabolism, glycerolipid metabolism and arginine biosynthesis. However, the pathway impact of CC exposure in the glycerolipid and gluthathione metabolism was very high. Likewise, after CC exposure and Se-supplementation (Fig. 4B) the same metabolic pathways were significantly altered with similar pathway impacts, when the metabolome is compared with C. Otherwise, when the testicular metabolome is compared between CC and CC-Se (Table S4), there are four significantly altered metabolic pathways, namely: aminoacyl-tRNA biosynthesis, purine metabolism, arginine biosynthesis and glycerolipid metabolism, and the last with an important pathway impact.

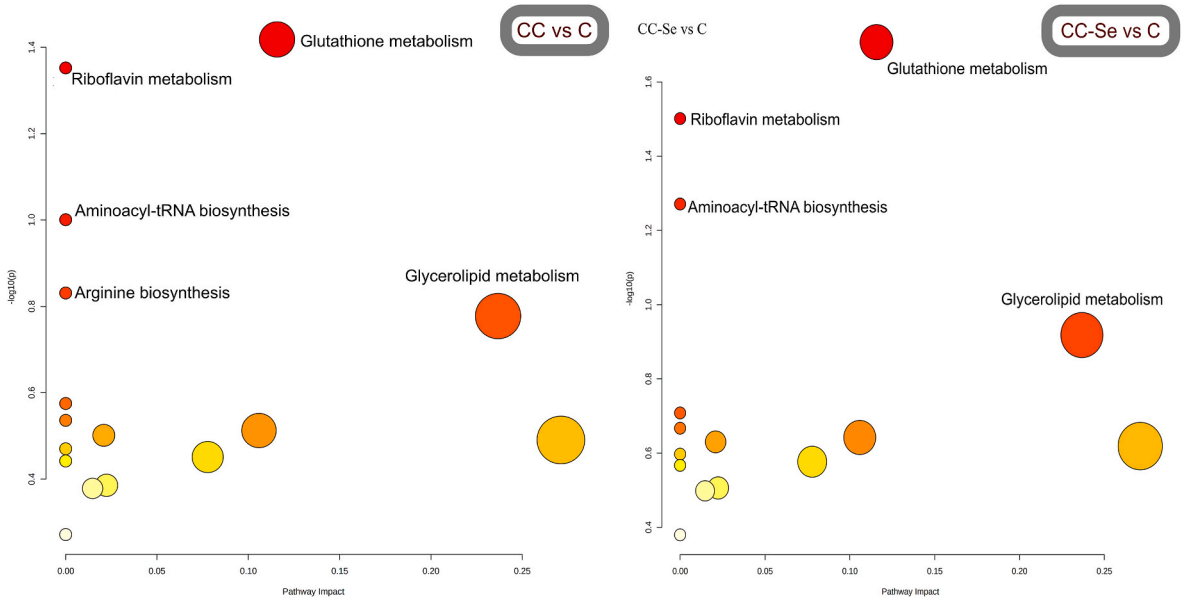

Fig. 4. (A) Pathway analysis plots showing the most impaired metabolic routes in CC and (B) CC-Se groups. The *p*-values calculated from the enrichment analysis are indicated by a color gradient: from white (highest *p*-value) to red (lowest *p*-value), while the pathway impact value calculated from pathway topology analysis is indicated by dot size. (For interpretation of the references to color in this figure legend, the reader is referred to the Web version of this article.)

3.2. Testicular metabolome is linked with gut microbiota and the associations are modulated by "chemical cocktail" exposure and selenium supplementation

Specific and significant links were found between the relative abundance of gut microbiota at the genus level and testicular metabolites in the different mice groups (Table S6, Figs. 5 and 6). Sixty-six genera with significantly different abundance among the studied mice groups were identified in mice gut microbiota (Table S5). These links between testicular metabolites and gut microbes present in the C group changed after CC exposure as well as by Se-supplementation. Thus, the microbial shifts can be classified as follows: (i) genera that present only links with testicular metabolites in C group (*e.g., Prevotellaceae UCG-001*, *Parvibacter*, *Oscillospiraceae UCG-005*, *Ruminococcaceae UBA1819*), (ii) genera that present only links with testicular metabolites in CC-Se group (*e.g., Clostridium innocuum group*, *Lachnospiraceae FCS020 group*, *Merdibacter*), (iii) genera that present links with testicular metabolites only in C and CC-Se group, but not in CC (*e.g., Rikenellaceae RC9 gut group*, *Streptococcus*, *Enterorhabdus*, *Anaerovoracaceae Family XIII UCG-001*), (iv) genera that present links with testicular metabolites only in CC and CC-Se groups, but not in C (*e.g.*, *Roseburia*, *Enterococcus, Erysipelatoclostridium, Anaeroplasma*, *Lachnospiraceae FCS020 group*, *Eubacterium siraeum group*, *Coriobacteriaceae UCG-002*, *Lachnospiraceae ASF356*, *Tuzzerella*). There were not any genus linked with testicular metabolites in CC group that were absent in the other groups.

The specific links between testicular metabolites and gut microbiota in CC and CC-Se groups are shown in Figs. 5 and 6, respectively. As can be seen, numerous links were shifted between both mice groups indicating a potential role of Se-supplementation in these associations. Thus, in CC group, *Roseburia* genus was negatively linked with testicular anandamide (20:1, n-9) and MG(16:1), while it was positively linked with calonectrin. However, after Se-supplementation (CC–Se), this genus was negatively linked with testicular FLQ and PS(16:0). *Lactobacillus* genus was negatively associated with PS(20:1), N-(14-methylhexadecanoyl)pyrrolidine, 16-hydroxy hexadecanoic acid and taurallocholic acid in CC group, while in CC-Se group, it was positively linked with stearidonyl carnitine and PG(16:0/16:0). Likewise, *Bacteroides* genus was negatively linked with lysoPE(16:0), 5-alpha-androstan-17-beta-ol propionate and 2-ethyl-1-hexanol sulfate inositol-scyllo in CC group, while in CC-Se group, it was positively linked with 5-deoxy-5-(methylthio)adenosine and negatively with pipericine. *Alloprevotella* was positively associated in CC group with flavin adenine dinucleotide (FAD) and negatively with phosphate, flumequine and pipericine, while in CC-Se group, it was negatively linked with anandamide (20:l, n-9), docosanamide, pipericine, and glycine and positively with flumequine, PS(16:0), LysoPE(20:4), 2-dodecylbenzenesulfonic acid, PG(16:0/16:0)

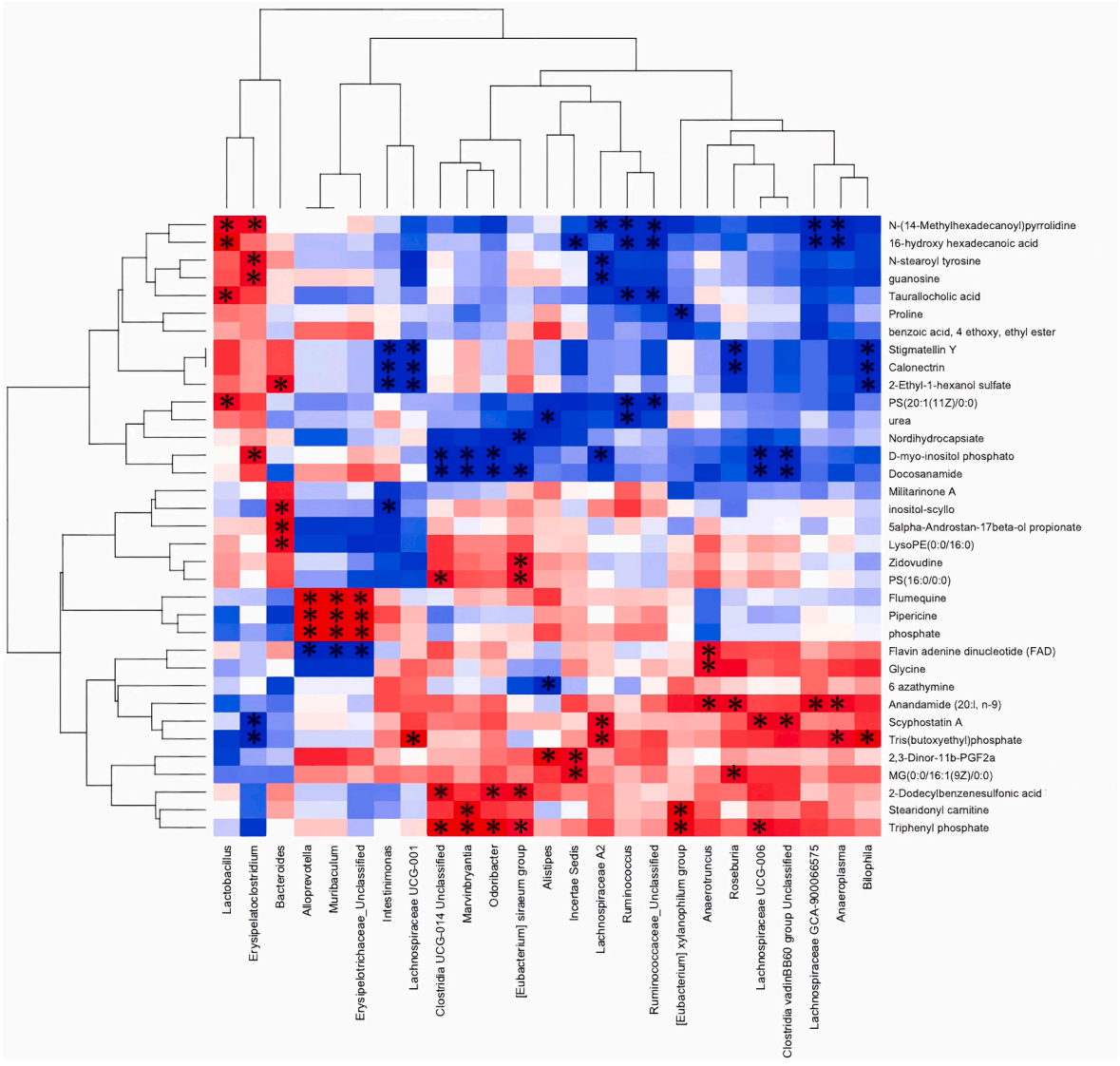

Fig. 5. Spearman correlation heatmaps showing the associations between testes metabolites and gut microbiota in CC.

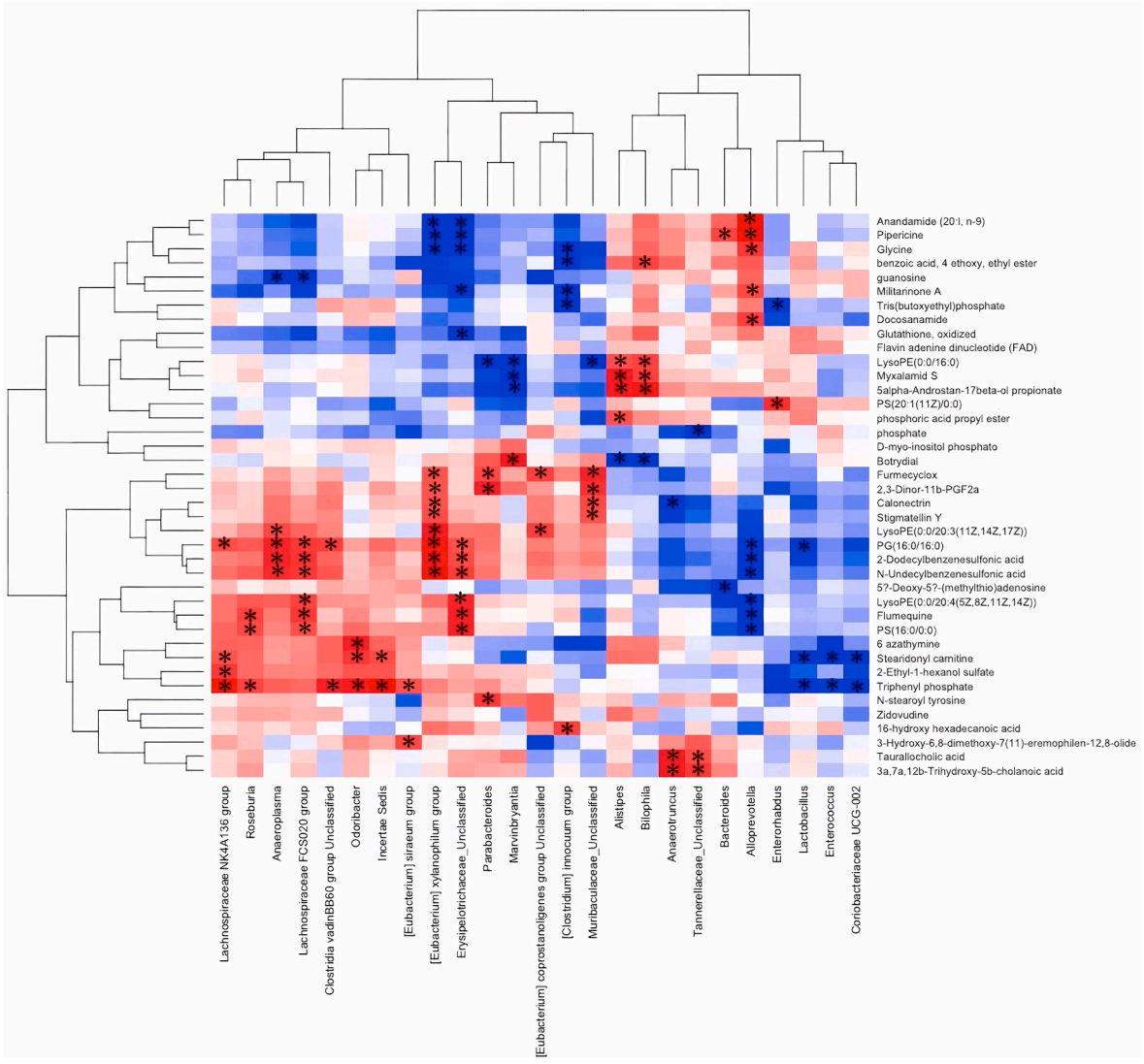

Fig. 6. Spearman correlation heatmaps showing the associations between testes metabolites and gut microbiota in CC-Se.

and N-undecylbenzenesulfonic acid. *Eubacterium xylanophilum* group was positively linked with proline, and D-myo-inositol phosphate in CC, while it was negatively with stearidonyl carnitine. However, in CC-Se it was positively linked with anandamide (20:1 n-9), pipericine and glycine, while it was negatively linked with LysoPE(20:3), 2,3-dinor-11b-PGF2a and 2-dodecylbenzenesulfonic acid.

4. Discussion

4.1. "Chemical cocktail" exposure and selenium supplementation modulated testicular metabolome

Our results suggest that the exposure to the "chemical cocktail" modulated mice testicular metabolome and that Se-supplementation restored many of them. Therefore, we found testicular metabolites only present in CC and CC-Se groups, but at significantly different levels when comparing both. This group of metabolites included FLQ, which was present in the "chemical cocktail" administered to the mice. The abundance of this metabolite was higher in the testicular tissue of mice from CC-Se when compared with CC (2.36-fold), suggesting that Se led to its accumulation in testicular tissue. In the same group of metabolites, Se led to a decrease of the steroid 5-alpha-androstan-17-beta-ol propionate (0.09-fold) in testis and an increase of nordihydrocapsiate and proline. Interestingly, the level of plasma 17-beta-hydroxy-5alpha-androstan-3-one (DHT) has been suggested as a parameter of androgenicity independent of testosterone (T) levels (Vermeulen, 1976), nordihydrocapsiate target specific metabolic pathways involved in inflammation and has shown potential health benefits (Sancho et al. n. d.) and proline improves haemato-biochemical and reproductive indicators in male rabbits affected by environmental stress (Abdelnour et al., 2021).

Moreover, CC led to the significant impairment of several metabolites, but their levels are comparable in the testicular tissues of mice from the C and CC-Se groups. Thus, suggesting a potential beneficial effect of Se-supplementation by restoring the levels of these molecules. Those testicular metabolites, which are all down-regulated after CC exposure, include the endogenous cannabinoid receptor ligand anandamide (20:l, n-9), that regulates gonadotropin releasing hormones in mammals (Battista et al., 2008), 2,3-dinor-11b-PGF2a, which is the most abundant metabolic product of prostaglandins released by activated mast cells and has been and is related with reproductive hormones (Sanyal et al., 1979), a neurotrophic compound (Riese et al., 2004) and PG (16:0/16:0). Our findings were according to Ramírez-Acosta et al. (2022), who also demonstrated the beneficial effects of dietary sodium selenite supplementation on mice reproductive health.

Testicular metabolomics revealed the unexpected presence of Ethyl

4-ethoxybenzoate, previously documented only in lactating female rats (Sreng et al., 2017), raising questions about its potential role in male reproductive function.

Se-supplementation also antagonized the up-or down-regulation of several metabolites altered by the exposure to the "chemical cocktail" like taurallocholic acid, a taurinated bile acid that beyond its role in digestion, impacts testicular physiology and male reproductive functions (Sèdes et al., 2017), and glycerol (Sèdes et al., 2017), which has antispermatogenic properties and when its levels are high in testis causes blood-testis barrier disruption, impairing tubular fluid homeostasis (Crisóstomo et al., 2017).

While Yang et al. (2022), focused on the time-dependent effects of pollutant exposure, our approach differed by capturing metabolic snapshots at one specific moment. This was motivated by the complexity of our animal model and instrumental limitations, which demanded a targeted analysis of one specific point of the exposure process.

In summary, CC altered mainly glutathione metabolism, aminoacyl-tRNA biosynthesis, riboflavin metabolism, glycerolipid metabolism and arginine biosynthesis and the Se-supplementation impact was mainly in the aminoacyl-tRNA biosynthesis, purine metabolism, arginine biosynthesis and especially, glycerolipid metabolism. Thus, comparing the two metabolic profiles we observed that one of the major differences at pathways levels was that riboflavin metabolism is not mainly affected under selenium supplementation. This finding is according to previous data (Wei et al., 2018) that confirm male infertility due to pollutants mediated by riboflavin metabolism impairment.

4.2. Testicular metabolites association with gut microbes and shifts induced by selenium supplementation

Our results revealed numerous links between gut microbiota and testicular metabolites suggesting a potential crosstalk induced by the exposure to the "chemical cocktail" and Se-supplementation. As commented before, some links are only present in C and CC-Se groups, but not in CC, suggesting a potential beneficial role of Se in the gut-gonad crosstalk. However, the testicular metabolites related to the specific gut microbiota, at the genus level, are different in the majority of the cases. Among these genera, there is a wide number of gut microbes that shifted the links with testicular metabolites when comparing CC and CC-Se groups. Among this bacteria, *Roseburia* genus has been previously correlated with seminal plasma metabolites in sheep with high-motility sperm (Wang et al., 2023), it was linked with testicular mice selenoproteins (Ramírez-Acosta et al., 2022), and it was negatively correlated with testosterone in mice (Liu et al., 2021), *Lactobacillus genus* down-regulates expression of cancer-testis genes (Azam et al., 2014), *Bacteroides* genus was reported to be one of the dominant genera in testicular maturing spermatozoa (Molina et al., 2021), *Alloprevotella* genus was positively correlated with testosterone in mice (Liu et al., 2021). *Eubacterium siraeum* has been associated with a wide range of diseases, indicating its potential role as microbial taxa with detrimental effects on the host. The altered abundance or activity of these bacteria, along with their metabolite production, may disrupt the delicate balance of the host-microbiota interaction and contribute to disease development or progression. The production of metabolites by these bacterial groups, which can include pro-inflammatory molecules or toxic byproducts, may further contribute to host harm.

In our previously published works, we determined the impact of Se-supplementation in plasma selenoproteins and gut microbiota (Callejón-Leblic et al., 2021), gut metabolites (Callejón-Leblic et al., 2022), brain metabolome (Ramírez-Acosta et al., 2023), testicular selenoproteins (Ramírez-Acosta et al., 2022) and interestingly, we found numerous associations between those selenoproteins and metabolites with specific gut microbes. Moreover, we described the impact of CC exposure on gut microbiota, plasma metabolome, plasma selenoproteins, and plasma arsenometabolites (Arias-Borrego et al., 2022) as well as brain metabolome (Parra-Martínez et al., 2022), demonstrating potential links between those molecules and gut microbiota. Regarding the potential antagonistic action of Se against pollutants, our previous results suggested that Se-supplementation led to the transport of almost all elements (except Cd) from less metabolic active organs (testes, brain, and lung) to the kidneys, probably stimulating the excretion and that Se and Cd co-exposure led to the accumulation of Cd in all the organs, but especially in testes (Rodríguez-Moro et al., 2020). The present work suggests the impact of "chemical cocktails" in the testicular metabolome and thus, in the gut-gonad crosstalk, as well as the influence of Se-supplementation on that.

4.2.1. Future perspectives

Our study provides novel insights into the role of pollutants and gut microbiota over mice testes metabolome. While our findings offer valuable information, further research is needed to address the specific and synergistic behavior of the different contaminants involved in our chemical cocktail. Additionally, our study used regular BALB/c mice which has certain limitations. Future studies could employ Germ-Free mice to further confirm and expand our gut microbiota-related findings. Ultimately, elucidating the role of microbiota in pollutant exposure could facilitate the development of more effective treatment strategies.

4.2.2. Limitations

Additionally, we were unable to control for all potential confounding factors, such as: understanding of the bioavailability and accumulations of the studied pollutants individually and as a cocktail, difficulties in accurately quantifying individual exposure levels, difficulties in the time–dependent effect of each pollutants and its synergistic effects, we are also affected by the challenges in metabolite identification and annotation. Future studies with more rigorous control of confounding variables and enhanced databases for metabolomics studies are needed to confirm and extend our findings.

5. Conclusions

Untargeted testicular metabolomics combining an analytical multi-platform based on GC-MS and UHPLC-QTOF-MS revealed an important impact of CC and a potential role of selenium supplementation as an antagonist. The annotated metabolites belongs to important class of compounds related to reproduction that have been reported to regulate gonadotropin releasing hormones in mammals, which are related with reproductive hormones. Thus, they impact on testicular physiology and on male reproductive functions, which has antispermatogenic properties and causes blood-testis barrier disruption, or that impairs tubular fluid homeostasis, among others. Our results also suggested an important "gut-gonad crosstalk" due to the great number of significant associations between gut microbes and testicular metabolites.

Funding sources

This work was supported by the projects: PID2021-123073NB-C21 from the Spanish Ministry of Science and Innovation (MICIN). Generación del Conocimiento. MCI/AEI/FEDER "Una manera de hacer Europa"; UHU-1256905 and UHU-202009 from the FEDER Andalusian Operative Program 2014–2020 (Ministry of Economy, Knowledge, Business and Universities, Regional Government of Andalusia, Spain). The authors are grateful to FEDER (European Community) for financial support, Grant UNHU13-1E-1611. CPM thanks MICIN for a predoctoral grant (ref. PRE2019-091,650). MSR and MCC also acknowledge the award of the Spanish Government MCIN/AEI to the Institute of Agrochemistry and Food Technology (IATA-CSIC) as Centre of Excellence Severo Ochoa (CEX2021-001189-S MCIN/AEI / 10.13039/501100011033). The authors would like to acknowledge the support from The Ramón Areces Foundation (ref. CIVP19A5918). Funding for open access charge: Universidad de Huelva/CBUA.

CRediT authorship contribution statement

C. Parra-Martínez: Writing – review & editing, Visualization, Validation, Investigation, Formal analysis, Data curation. **M. Selma-Royo:** Writing – review & editing, Investigation, Formal analysis, Data curation. **B. Callejón-Leblic:** Writing – review & editing, Supervision, Formal analysis, Data curation. **M.C. Collado:** Writing – review & editing, Writing – original draft, Visualization, Supervision, Resources, Project administration, Methodology, Investigation, Funding acquisition, Conceptualization. **N. Abril:** Writing – review & editing, Writing – original draft, Methodology, Investigation, Funding acquisition, Conceptualization, Validation, Visualization. **T. García-Barrera:** Project administration, Methodology, Investigation, Funding acquisition, Conceptualization, Resources, Supervision, Visualization, Writing – original draft, Writing – review & editing.

Declaration of competing interest

The authors declare that they have no known competing financial interests or personal relationships that could have appeared to influence the work reported in this paper.

Data availability

Data will be made available on request.

Abbreviations

C	control mice group fed regular rodent diet
CC	mice fed regular diet exposed to the chemical cocktail
CC-Se	mice fed Se supplemented diet exposed to the chemical cocktail
KRI	Kovat's retention indexes
FC	Fold change
PE	phosphatidylethanolamine
PS	phosphatidylserine
PG	Phosphatidylglycerol
MG	Monoacylglycerol
QC	quality control samples
PLS-Das	partial least squares discriminant analysis
PCA	Principal Components Analysis
MTBE	Methyl tertiary-butyl ether
DCF	diclofenac
FLQ	flumequine
GC-MS	gas chromatography-mass spectrometry
UHPLC-QTOF	ultra-high performance liquid chromatography coupled to quadrupole time of flight
TMS	trimethylsilyl
FC	fold-changes
PCAs	polycyclic aromatic compounds
As	arsenic
Hg	Mercury
Cd	Cadmium
Se	Selenium
Sb	antimony

Appendix A. Supplementary data

Supplementary data to this article can be found online at https://doi.org/10.1016/j.fct.2024.114627.

References

Abdelnour, S.A., Al-Gabri, N.A., Hashem, N.M., Gonzalez-Bulnes, A., 2021. Supplementation with proline improves haemato-biochemical and reproductive indicators in male rabbits affected by environmental Heat-stress. Anim. an open access J. from MDPI 11, 1–15. https://doi.org/10.3390/ANI11020373.

Arias-Borrego, A., Selma-Royo, M., Collado, M.C., Abril, N., García-Barrera, T., 2022. Impact of 'chemical cocktails' exposure in shaping mice gut microbiota and the role of selenium supplementation combining metallomics, metabolomics, and metataxonomics. J. Hazard Mater. 438 https://doi.org/10.1016/J.JHAZMAT.2022.129444.

Azam, R., Ghafouri-Fard, S., Tabrizi, M., Modarressi, M.H., Ebrahimzadeh-Vesal, R., Daneshvar, M., Mobasheri, M.B., Motevaseli, E., 2014. Lactobacillus acidophilus and Lactobacillus crispatus culture supernatants downregulate expression of cancer-testis genes in the MDA-MB-231 cell line. Asian Pac. J. Cancer Prev. 15, 4255–4259. https://doi.org/10.7314/APJCP.2014.15.10.4255.

Battista, N., Rapino, C., Di Tommaso, M., Bari, M., Pasquariello, N., Maccarrone, M., 2008. Regulation of male fertility by the endocannabinoid system. Mol. Cell. Endocrinol. 286 https://doi.org/10.1016/J.MCE.2008.01.010.

Cai, X., Wang, C., Yu, W., Fan, W., Wang, S., Shen, N., Wu, P., Li, X., Wang, F., 2016. Selenium exposure and cancer risk: an updated meta-analysis and meta-regression. Sci. Rep. 6 https://doi.org/10.1038/SREP19213.

Callejón-Leblic, B., Selma-Royo, M., Collado, M.C., Abril, N., García-Barrera, T., 2021. Impact of antibiotic-induced depletion of gut microbiota and selenium supplementation on plasma selenoproteome and metal homeostasis in a mice model. J. Agric. Food Chem. 69, 7652–7662. https://doi.org/10.1021/ACS.JAFC.1C02622.

Callejón-Leblic, B., Selma-Royo, M., Collado, M.C., Gómez-Ariza, J.L., Abril, N., García-Barrera, T., 2022. Untargeted gut metabolomics to delve the interplay between selenium supplementation and gut microbiota. J. Proteome Res. 21, 758–767. https://doi.org/10.1021/ACS.JPROTEOME.1C00411.

Crisóstomo, L., Alves, M.G., Calamita, G., Sousa, M., Oliveira, P.F., 2017. Glycerol and testicular activity: the good, the bad and the ugly. Mol. Hum. Reprod. 23, 725–737. https://doi.org/10.1093/MOLEHR/GAX049.

D'Amato, A., Di Cesare Mannelli, L., Lucarini, E., Man, A.L., Le Gall, G., Branca, J.J.V., Ghelardini, C., Amedei, A., Bertelli, E., Regoli, M., Pacini, A., Luciani, G., Gallina, P., Altera, A., Narbad, A., Gulisano, M., Hoyles, L., Vauzour, D., Nicoletti, C., 2020. Faecal microbiota transplant from aged donor mice affects spatial learning and memory via modulating hippocampal synaptic plasticity- and neurotransmission-related proteins in young recipients. Microbiome 8. https://doi.org/10.1186/S40168-020-00914-W.

da Silva, R.F., Borges, C., dos, S., Lamas, C. de A., Cagnon, V.H.A., Kempinas, W. de G., 2017. Arsenic trioxide exposure impairs testicular morphology in adult male mice and consequent fetus viability. J. Toxicol. Environ. Health 80, 1166–1179. https://doi.org/10.1080/15287394.2017.1376405.

De Geyter, C., Calhaz-Jorge, C., Kupka, M.S., Wyns, C., Mocanu, E., Motrenko, T., Scaravelli, G., Smeenk, J., Vidakovic, S., Goossens, V., Gliozheni, O., Strohmer, H., Petrovskaya, E., Tishkevich, O., Bogaerts, K., Balic, D., Sibincic, S., Antonova, I., Vrcic, H., Ljiljak, D., Pelekanos, M., Rezabek, K., Markova, M.J., Lemmen, J., Sõritsa, D., Gissler, M., Tiitinen, A., Royere, D., Tandler—schneider, A., Kimmel, M., Antsaklis, A.J., Loutradis, D., Urbancsek, J., Kosztolanyi, G., Bjorgvinsson, H., de Luca, R., Lokshin, V., Ravil, V., Magomedova, V., Gudleviciene, Z., Belo Lopes, G., Petanovski, Z., Calleja-Agius, J., Xuereb, J., Moshin, V., Simic, T.M., Vukicevic, D., Romundstad, L.B., Janicka, A., Laranjeira, A.R., Rugescu, I., Doroftei, B., Korsak, V., Radunovic, N., Tabs, N., Virant-Klun, I., Saiz, I.C., Mondéjar, F.P., Bergh, C., Weder, M., Smeenk, J.M.J., Gryshchenko, M., Baranowski, R., 2018. ART in Europe, 2014: results generated from European registries by ESHRE: the European IVF-monitoring consortium (EIM) for the European society of human reproduction and embryology (ESHRE). Hum. Reprod. 33, 1586–1601. https://doi.org/10.1093/HUMREP/DEY242.

Fekadu, S., Alemayehu, E., Dewil, R., Van der Bruggen, B., 2019. Pharmaceuticals in freshwater aquatic environments: a comparison of the African and European challenge. Sci. Total Environ. 654, 324–337. https://doi.org/10.1016/J.SCITOTENV.2018.11.072.

Gao, Y., Mruk, D.D., Cheng, C.Y., 2015. Sertoli cells are the target of environmental toxicants in the testis - a mechanistic and therapeutic insight. Expert Opin. Ther. Targets 19, 1073–1090. https://doi.org/10.1517/14728222.2015.1039513.

García-Barrera, T., Gómez-Ariza, J.L., González-Fernández, M., Moreno, F., García-Sevillano, M.A., Gómez-Jacinto, V., 2012. Biological responses related to agonistic, antagonistic and synergistic interactions of chemical species. Anal. Bioanal. Chem. 403, 2237–2253. https://doi.org/10.1007/S00216-012-5776-2.

García-Sevillano, M.Á., García-Barrera, T., Abril, N., Pueyo, C., López-Barea, J., Gómez-Ariza, J.L., 2014a. Omics technologies and their applications to evaluate metal toxicity in mice M. spretus as a bioindicator. J. Proteonomics 104, 4–23. https://doi.org/10.1016/J.JPROT.2014.02.032.

García-Sevillano, M.Á., García-Barrera, T., Navarro-Roldán, F., Montero-Lobato, Z., Gómez-Ariza, J.L., 2014b. A combination of metallomics and metabolomics studies to evaluate the effects of metal interactions in mammals. Application to Mus musculus mice under arsenic/cadmium exposure. J. Proteonomics 104, 66–79. https://doi.org/10.1016/J.JPROT.2014.02.011.

García-Sevillano, M.A., García-Barrera, T., Navarro, F., Gailer, J., Gómez-Ariza, J.L., 2014. Use of elemental and molecular-mass spectrometry to assess the toxicological effects of inorganic mercury in the mouse Mus musculus. Anal. Bioanal. Chem. 406, 5853–5865. https://doi.org/10.1007/S00216-014-8010-6.

García-Sevillano, M.A., García-Barrera, T., Navarro, F., Gómez-Ariza, J.L., 2013a. Analysis of the biological response of mouse liver (Mus musculus) exposed to As2O3 based on integrated -omics approaches. Metallomics 5, 1644–1655. https://doi.org/10.1039/C3MT00186E.

García-Sevillano, M.A., Jara-Biedma, R., González-Fernández, M., García-Barrera, T., Gómez-Ariza, J.L., 2013b. Metal interactions in mice under environmental stress. Biometals 26, 651–666. https://doi.org/10.1007/S10534-013-9642-2.

Gómez-Jacinto, V., García-Barrera, T., Garbayo, I., Vílchez, C., Gómez-Ariza, J.L., 2012. Metallomic study of selenium biomolecules metabolized by the microalgae Chlorella

sorkiniana in the biotechnological production of functional foods enriched in selenium. Pure Appl. Chem. 84, 269–280. https://doi.org/10.1351/PAC-CON-11-09-18/MACHINEREADABLECITATION/RIS.

González-Gaya, B., García-Bueno, N., Buelow, E., Marin, A., Rico, A., 2022. Effects of aquaculture waste feeds and antibiotics on marine benthic ecosystems in the Mediterranean Sea. Sci. Total Environ. 806 https://doi.org/10.1016/J.SCITOTENV.2021.151190.

Huygens, J., Rasschaert, G., Heyndrickx, M., Dewulf, J., Van Coillie, E., Quataert, P., Daeseleire, E., Becue, I., 2022. Impact of fertilization with pig or calf slurry on antibiotic residues and resistance genes in the soil. Sci. Total Environ. 822 https://doi.org/10.1016/J.SCITOTENV.2022.153518.

Jarak, I., Almeida, S., Carvalho, R.A., Sousa, M., Barros, A., Alves, M.G., Oliveira, P.F., 2018. Senescence and declining reproductive potential: insight into molecular mechanisms through testicular metabolomics. Biochim. Biophys. Acta (BBA) - Mol. Basis Dis. 1864 (10), 3388–3396. https://doi.org/10.1016/j.bbadis.2018.07.028.

Kilchevsky, A., Honig, S., 2012. Semen quality, sperm selection and hematospermia. Nat. Rev. Urol. 92 (9), 68–70. https://doi.org/10.1038/nrurol.2011.234.

Li, S., Han, B., Wu, P., Yang, Q., Wang, X., Li, J., Liao, Y., Deng, N., Jiang, H., Zhang, Z., 2022. Effect of inorganic mercury exposure on reproductive system of male mice: immunosuppression and fibrosis in testis. Environ. Toxicol. 37, 69–78. https://doi.org/10.1002/TOX.23378.

Liu, L., Shu, A., Zhu, Y., Chen, Y., 2021. Cornuside alleviates diabetes mellitus-induced testicular damage by modulating the gut microbiota. Evid. Based. Complement. Alternat. Med. https://doi.org/10.1155/2021/5301942.

Minutoli, L., Micali, A., Pisani, A., Puzzolo, D., Bitto, A., Rinaldi, M., Pizzino, G., Irrera, N., Galfo, F., Arena, S., Pallio, G., Mecchio, A., Germanà, A., Bruschetta, D., Laurà, R., Magno, C., Marini, H., Squadrito, F., Altavilla, D., 2015. Flavocoxid protects against cadmium-induced disruption of the blood–testis barrier and improves testicular damage and germ cell impairment in mice [corrected]. Toxicol. Sci. 148, 311–329. https://doi.org/10.1093/TOXSCI/KFV185.

Molina, N.M., Plaza-Díaz, J., Vilchez-Vargas, R., Sola-Leyva, A., Vargas, E., Mendoza-Tesarik, R., Galán-Lázaro, M., Mendoza-Ladrón de Guevara, N., Tesarik, J., Altmäe, S., 2021. Assessing the testicular sperm microbiome: a low-biomass site with abundant contamination. Reprod. Biomed. Online 43, 523–531. https://doi.org/10.1016/J.RBMO.2021.06.021.

Orisakwe, O.E., Afonne, O.J., Nwobodo, E., Asomugha, L., Dioka, C.E., 2001. Low-dose mercury induces testicular damage protected by zinc in mice. Eur. J. Obstet. Gynecol. Reprod. Biol. 95, 92–96. https://doi.org/10.1016/S0301-2115(00)00374-2.

Owumi, S.E., Aliyu-Banjo, N.O., Odunola, O.A., 2020. Selenium attenuates diclofenac-induced testicular and epididymal toxicity in rats. Andrologia 52. https://doi.org/10.1111/AND.13669.

Parra-Martínez, C., Selma-Royo, M., Callejón-Leblic, B., Collado, M.C., Abril, N., García-Barrera, T., 2022. Mice brain metabolomics after the exposure to a 'chemical cocktail' and selenium supplementation through the gut-brain axis. J. Hazard Mater. 438 https://doi.org/10.1016/J.JHAZMAT.2022.129443.

Ramírez-Acosta, S., Arias-Borrego, A., Navarro-Roldán, F., Selma-Royo, M., Calatayud, M., Collado, M.C., Huertas-Abril, P.V., Abril, N., Barrera, T.G., 2021. Omic methodologies for assessing metal(-loid)s-host-microbiota interplay: a review. Anal. Chim. Acta 1176, 338620. https://doi.org/10.1016/J.ACA.2021.338620.

Ramírez-Acosta, S., Huertas-Abril, P.V., Selma-Royo, M., Prieto-Álamo, M.J., Collado, M. C., Abril, N., García-Barrera, T., 2023. The role of selenium in shaping mice brain metabolome and selenoproteome through the gut-brain axis by combining metabolomics, metallomics, gene expression and amplicon sequencing. J. Nutr. Biochem. 109323 https://doi.org/10.1016/J.JNUTBIO.2023.109323.

Ramírez-Acosta, S., Selma-Royo, M., Collado, M.C., Navarro-Roldán, F., Abril, N., García-Barrera, T., 2022. Selenium supplementation influences mice testicular selenoproteins driven by gut microbiota. Sci. Rep. 12 https://doi.org/10.1038/S41598-022-08121-3.

Riese, U., Ziegler, E., Hamburger, M., 2004. Militarinone A induces differentiation in PC12 cells via MAP and Akt kinase signal transduction pathways. FEBS Lett. 577, 455–459. https://doi.org/10.1016/j.febslet.2004.10.045.

Rodríguez-Moro, G., Abril, N., Jara-Biedma, R., Ramírez-Acosta, S., Gómez-Ariza, J.L., Garciá-Barrera, T., 2019. Metabolic impairments caused by a 'chemical cocktail' of DDE and selenium in mice using direct infusion triple quadrupole time-of-flight and gas chromatography-mass spectrometry. Chem. Res. Toxicol. 32, 1940–1954. https://doi.org/10.1021/ACS.CHEMRESTOX.9B00102.

Rodríguez-Moro, G., Roldán, F.N., Baya-Arenas, R., Arias-Borrego, A., Callejón-Leblic, B., Gómez-Ariza, J.L., García-Barrera, T., 2020. Metabolic impairments, metal traffic, and dyshomeostasis caused by the antagonistic interaction of cadmium and selenium using organic and inorganic mass spectrometry. Environ. Sci. Pollut. Res. Int. 27, 1762–1775. https://doi.org/10.1007/S11356-019-06573-1.

Sancho, R., on Lucena, C., Macho, A., Calzado, M.A., Blanco-Molina, M., Minassi, A., Appendino, G., MuñozMu, E., n.d. Immunosuppressive activity of capsaicinoids: capsiate derived from sweet peppers inhibits NF-⟨ B activation and is a potent antiinflammatory compound in vivo. https://doi.org/10.1002/1521-4141(200206)32:6.

Sanyal, S., Deb, C., Patra, P.B., Biswas, N.M., 1979. In vitro studies on histochemical localization of testicular delta5-3beta-hydroxysteroid dehydrogenase activity from indomethacin pretreated rats–effect of prostaglandins and luteinizing hormone. Andrologia 11, 157–162. https://doi.org/10.1111/J.1439-0272.1979.TB02180.X.

Sarkar, S., Hazra, J., Upadhyay, S.N., Singh, R.K., Chowdhury, A.R., 2008. Arsenic induced toxicity on testicular tissue of mice. Indian J. Physiol. Pharmacol. 52, 84–90.

Sèdes, L., Martinot, E., Baptissart, M., Baron, S., Caira, F., Beaudoin, C., Volle, D.H., 2017. Bile acids and male fertility: from mouse to human? Mol. Aspect. Med. 56, 101–109. https://doi.org/10.1016/J.MAM.2017.05.004.

Sreng, L., Temime-Roussel, B., Wortham, H., Mourre, C., 2017. Chemical identification of "maternal signature odors" in rat. Chem. Senses 42 (3), 211–222. https://doi.org/10.1093/chemse/bjw124.

Vermeulen, A., 1976. Testosterone and 5alpha-androstan-17beta-ol-3-one (DHT) levels in man. Acta Endocrinol. 83, 651–654. https://doi.org/10.1530/ACTA.0.0830651.

Wang, M., Ren, C., Wang, P., Cheng, X., Chen, Y., Huang, Y., Chen, J., Sun, Z., Wang, Q., Zhang, Z., 2023. Microbiome-metabolome reveals the contribution of the gut-testis Axis to sperm motility in sheep (Ovis aries). Anim. an open access J. from MDPI 13, 996. https://doi.org/10.3390/ANI13060996.

Wei, Z., Xi, J., Gao, S., You, X., Li, N., Cao, Y., et al., 2018. Metabolomics coupled with pathway analysis characterizes metabolic changes in response to BDE-3 induced reproductive toxicity in mice. Sci. Rep. 8 (1), 5423. https://doi.org/10.1038/s41598-018-23484-2.

Wu, S., Zhong, G., Wan, F., Jiang, X., Tang, Z., Hu, T., Rao, G., Lan, J., Hussain, R., Tang, L., Zhang, H., Huang, R., Hu, L., 2021. Evaluation of toxic effects induced by arsenic trioxide or/and antimony on autophagy and apoptosis in testis of adult mice. Environ. Sci. Pollut. Res. Int. 28, 54647–54660. https://doi.org/10.1007/S11356-021-14486-1.

Yang, J., Liao, A., Hu, S., Zheng, Y., Liang, S., Han, S., Lin, Y., 2022. Acute and chronic toxicity of binary mixtures of bisphenol A and heavy metals, 2022 Toxics 10, 255. https://doi.org/10.3390/toxics10050255. Aquatic Emerging Contaminants and Their Ecotoxicological Consequences, 115.

Zarrinpar, A., Chaix, A., Xu, Z.Z., Chang, M.W., Marotz, C.A., Saghatelian, A., Knight, R., Panda, S., 2018. Antibiotic-induced microbiome depletion alters metabolic homeostasis by affecting gut signaling and colonic metabolism. Nat. Commun. 9 https://doi.org/10.1038/S41467-018-05336-9.